

Elongation determination using finite element and boundary element method

Piotr Kisala, Waldemar Wójcik, Nurzhigit Smailov, Aliya Kalizhanova and Damian Harasim

Abstract—This paper presents an application of the finite element method and boundary element method to determine the distribution of the elongation. Computer simulations were performed using the computation of numerical algorithms according to a mathematical structure of the model and taking into account the values of all other elements of the fiber Bragg grating (FBG) sensor. Experimental studies were confirmed by elongation measurement system using one uniform FBG.

Keywords—finite element method, boundary element method, fiber Bragg gratings, elongation distribution

I. INTRODUCTION

ELONGATION measurement are very important in many practical cases [1]. Many differential speed measurement algorithms was introduced, showing how to solve eccentricity problems and that a bad processing but not slippage is the source of observed false elongation peaks [2]. In some cases the elongation sensor using optical elements is used [3-5]. A two-dimensional formulation within the scope of the boundary element method (BEM) was proposed for the determination of influence of shear and elongation on drop deformation [6]. Sometimes the Indirect Boundary Element Method (IBEM) is applied for the strain calculations eg. to study composites models [7] and scattering of elastic waves by cracks [8]. The finite element method is also widely used for the elongation determination [9], eg. in modeling and simulation of porcine liver tissue indentation [10] elasticity and fracture analysis [11] and also in many mechanical systems [12]. An efficient hybrid approach to study the deformation in known materials have been presented in our method. In this work the relative elongation is determined for the formed mechanical system using finite element method (FEM) and boundary element method. In addition, the results have been verified by measurements using FBG sensor. In this paper, the inverse problem solution is used to estimate the model parameters of elongation sensor in accordance with the method of measuring the elongation distribution [13,14]. To confirm the results obtained from FEM and BEM, measurements using FBG sensor have been performed. During measurements of the

elongation distribution using inverse analysis it is important to build sensor model [15-17]. Direct measurements of described quantity are not possible due to lack of appropriate measurement system components (especially sensors), therefore the measurements are indirect [18-22]. In this case, it is essential to the use of optoelectronic devices, which process the available physical signals using specialized sensors, converts them into digital form, and then, according to the implemented numerical algorithms, converts it to the desirable quantity. In this paper we present an application of the finite element method and boundary element method to determine the distribution of the elongation and we implement the inverse analysis to the elongation determination.

II. CALCULATION METHOD AND MEASUREMENT SYSTEM

The elongation distribution of the sample material can be determined based on the distribution of the linear dimensions relative change in the considered area. The study lead to the use of information from the measured spectrum and the spectrum calculated by use of mathematical model. To perform the experiments laboratory testing tool was designed and manufactured. It allows for the metal specimens stretching. Bragg gratings were glued on the specimens. Elongation of the sample, moving into a grating, causing changes in the length of the grating period, which also changes its spectral characteristics, which possible to determine with photo spectrometer. The spectral characteristics of the grating allows to obtain the information about the elongation distribution even repeatedly differential along the measured length. Knowing the cross-section of the sample and the load the elongation was calculated at several points. For the calculation the finite element method and the boundary element method were used. FEM mesh is arranged in such a way that its greatest density occurred on the sample constriction. However, in the BEM the values of elongation were calculated on the external and internal edge of the specimen on its constriction.

Light with wavelengths of 400-1700 nm is directed to an optical fiber in which the Bragg grating is written. The grating was glued to the sample, which is under tensile force F using the laboratory strain generator. After passing through an extended grating the modified spectrum is directed to an optical spectrum analyzer. At the same time the random distribution of the elongation is generated using simulated annealing algorithm. This random distribution is then introduced into the Bragg grating model. Presented method is shown in Figure 1.

P. Kisala, W. Wójcik, D. Harasim are with the Lublin University of Technology, Institute of Electronics and Information Technology, Lublin, Poland (email: p.kisala@pollub.pl, waldemar.wojcik@pollub.pl, d.harasim@pollub.pl).

N. Smailov, A. Kalizhanova are with the Kazakh National Research Technical University after K. I. Satpaev, Kazakhstan (email: nur_aly.kz@mail.ru, kalizhanova_aliya@mail.ru).

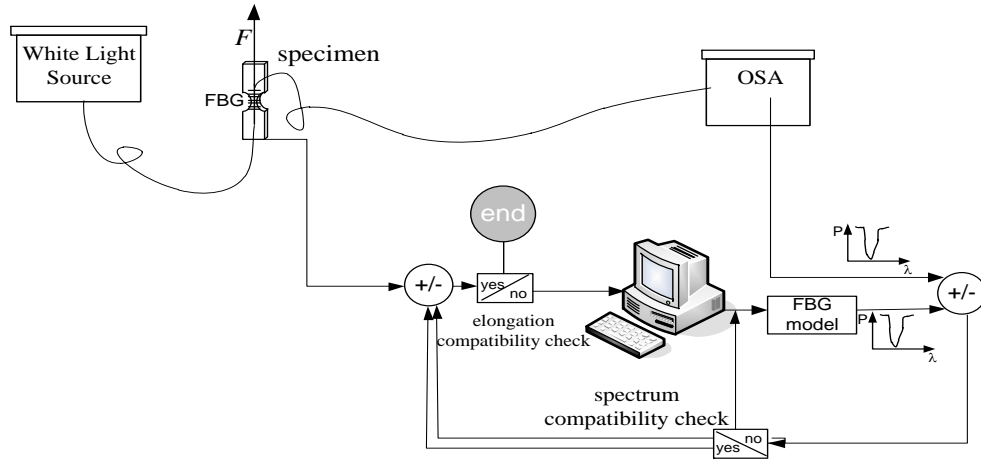


Figure 1. Elongation determination system on the base of FBG model

By means of a model and on the base of random elongation distribution the transmission spectrum of the grating is calculated. The modeled spectrum and actual spectrum (from optical spectrum analyzer - OSA) are then compared. In the case of spectral characteristics non-compliance, new values of the grating elongation distribution are selected in accordance with the simulated annealing algorithm. These are re-used to calculate a new transmission spectrum by means of a grating model. It is compared with the measured spectrum and the process is repeated until a predetermined accuracy is achieved or until a specified (suitably small) value of the objective

function is achieved. Distribution of elongation, which will lead to the minimization of the objective function will be the most fitting for real. The next step is to check the compliance of the distribution determined using an algorithm with the theoretical one, resulting from tensile force F and the shape of the stretched specimen. Knowledge of the force F and the shape of the specimen allows for calculation (using the FEM and BEM) the theoretical elongation distribution of the specimen and the grating. Fig. 2 shows the measurement system components.

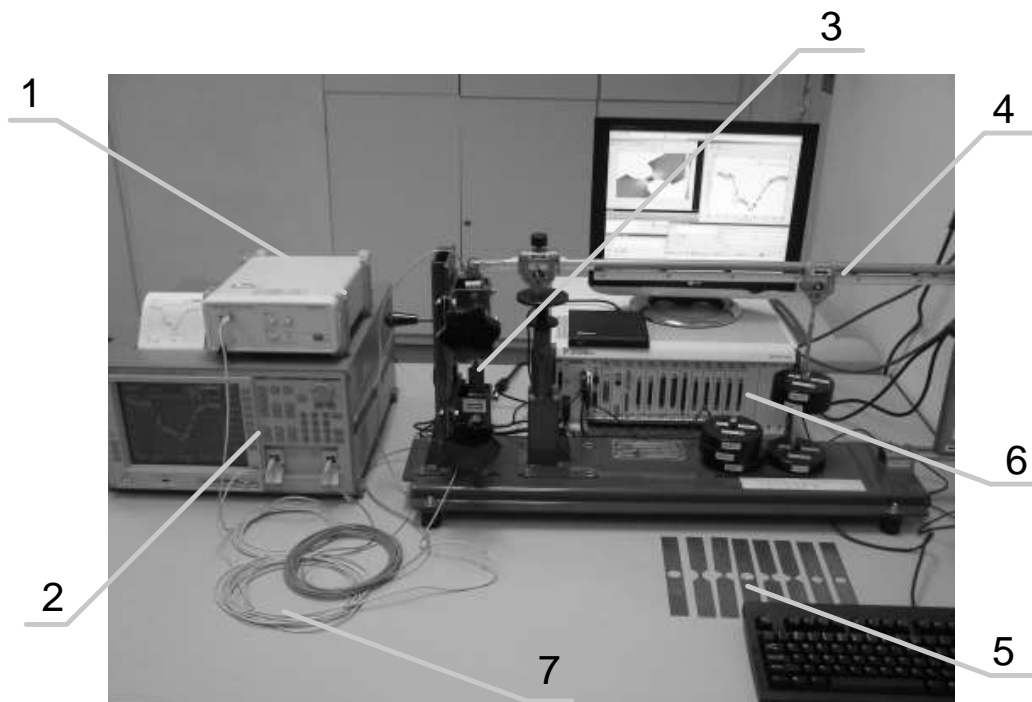


Figure 2. Measurement system: 1 – light source, 2 – optical spectrum analyser, 3 – Bragg grating, 4 – elongation generator, 5 – specimens, 6 - PC with measuring card, 7 – optical fiber with FBG

The coupled-mode equations were used in the simulation of the spectral response of the Bragg grating. The white light is the sensor model input. The input can be expressed as $R(-L/2)$. The output of the model is the light transmitted through the grating (grating's transmission spectrum), which can be expressed as $R(+L/2)$. The model parameters are as follows: the grating length L , the "DC" self-coupling coefficient σ , and the coupling coefficient k . There is no input signal that is incident from the right-hand side of the grating, i.e. $S(+L/2)=0$, but there is a known signal value that is incident from the left side of the grating, i.e. $R(-L/2)=1$ (Fig. 3).

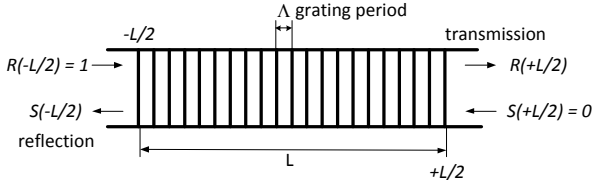


Figure 3. The initial condition and calculation of the grating response to input field

The grating is represented by the transfer matrix F_M . The light propagation process can be described by:

$$\begin{bmatrix} R(+L/2) \\ S(-L/2) \end{bmatrix} = F_M \cdot \begin{bmatrix} R(-L/2) \\ S(+L/2) \end{bmatrix}. \quad (1)$$

$S(-L/2)$ is the signal reflected from the grating and the F_M matrix can be expressed as follows:

$$F_M = \begin{bmatrix} \cosh(\gamma_B L) - i \frac{\sigma}{\gamma_B} \sinh(\gamma_B L) & -i \frac{k}{\gamma_B} \sinh(\gamma_B L) \\ i \frac{k}{\gamma_B} \sinh(\gamma_B L) & \cosh(\gamma_B L) + i \frac{\sigma}{\gamma_B} \sinh(\gamma_B L) \end{bmatrix}. \quad (2)$$

The individual elements of the F_M matrix can be described as follows. The general "DC" self-coupling coefficient σ can be represented by:

$$\sigma = \delta + \bar{\sigma} - \frac{1}{2} \frac{d\phi}{dz},$$

where $\frac{1}{2} \frac{d\phi}{dz}$ describes a possible chirp of the grating period, and ϕ is the grating phase. The detuning parameter δ can be represented by:

$$\delta = \beta - \frac{\pi}{\lambda} = \beta - \beta_D = 2\pi n_{eff} \left(\frac{1}{\lambda} - \frac{1}{\lambda_D} \right), \quad (4)$$

where $\lambda_D = 2n_{eff} \Lambda$ is the design wavelength for Bragg

reflectance. For very weak gratings where $(\delta n_{eff} \rightarrow 0)$ we obtain:

$$\bar{\sigma} = \frac{2\pi}{\lambda} \overline{\delta n_{eff}}, \quad (5)$$

where $\overline{\delta n_{eff}}$ is the background refractive index change. The coupling coefficient $k(z)$ can be represented by:

$$k(z) = \frac{\pi}{\lambda} \delta n(z) g(z) \nu, \quad (6)$$

where $g(z)$ is the function of apodization, and ν is the fringe visibility. The coupling coefficient $k(z)$ is proportional to the modulation depth of the refractive index $\Delta n(z) = \delta n(z) g(z)$.

In our case the grating was apodized and the apodization profile was given by the grating producer. The simulated grating apodization function was as follows:

$$g(z) = \exp \left[-a \left(\frac{z - \frac{L}{2}}{L} \right)^2 \right]; \quad z \in [0, L], \quad (7)$$

where a is the Gauss function width parameter and in our case $a = 80$. γ_B can be expressed by the following equations:

$$\gamma_B = \sqrt{k^2 - \sigma^2} \quad k^2 > \sigma^2, \quad (8)$$

$$\gamma_B = i\sqrt{\sigma^2 - k^2} \quad k^2 < \sigma^2, \quad (9)$$

The grating FBG2 can be represented by a single transfer matrix describing its entire length because we assume a uniform temperature along the entire grating. There is therefore no need for the transfer function of light passing through FBG2 to depend on the position along the z axis. This assumption simplifies the mathematical model.

III. CALCULATION METHOD AND MEASUREMENT RESULTS

In Fig. 4 a shape of a used specimen has been presented, Fig. 5 presents elongation distribution of the specimen as a function of stress calculated on the basis of knowledge of the load, the specimen geometry and the type of material using MES and simulated (determined from indirect measurements on a laboratory). In contrast, in Fig. 6 the distribution of elongation for the same specimen as a function of stress using the boundary element method has been presented.

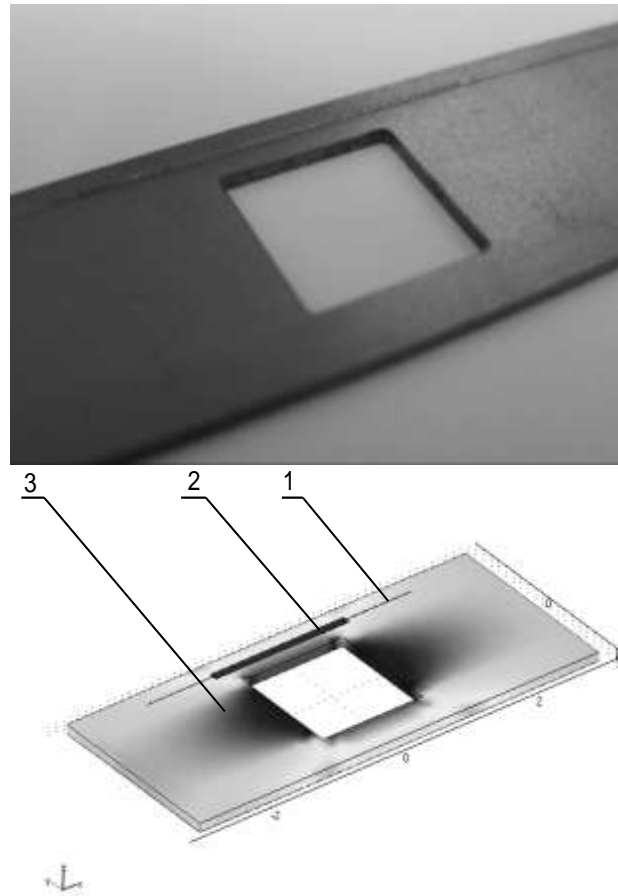


Figure 4. Measured system: 1 –optical fiber with FBG, 2 –epoxy glue, 3 – specimen.
a) real photo, b) system geometry in FEM

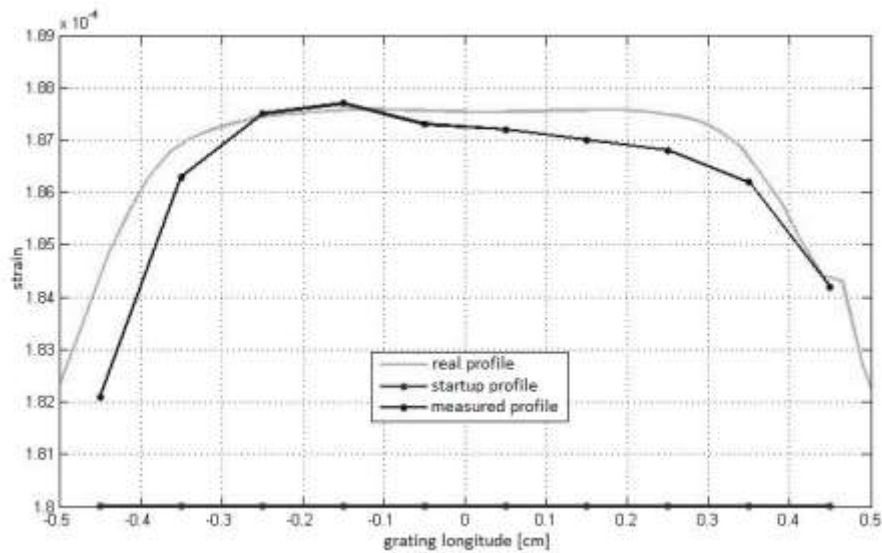


Figure 5. Distributions of elongation in FBG

In Fig. 4 elongation distribution characteristics of the Bragg grating have been presented. The profile determined as real was calculated using finite element method. The known tensile force and geometry of the specimen were used as the input quantities. The profile determined as measured was determined using Bragg gratings spectra, FBG model and

simulated annealing algorithm. The algorithm does not know the force size and the specimen geometry. The process of determining the elongation distribution of Bragg grating began with a random initial value of tension, which was assumed constant throughout the length of the specimen.

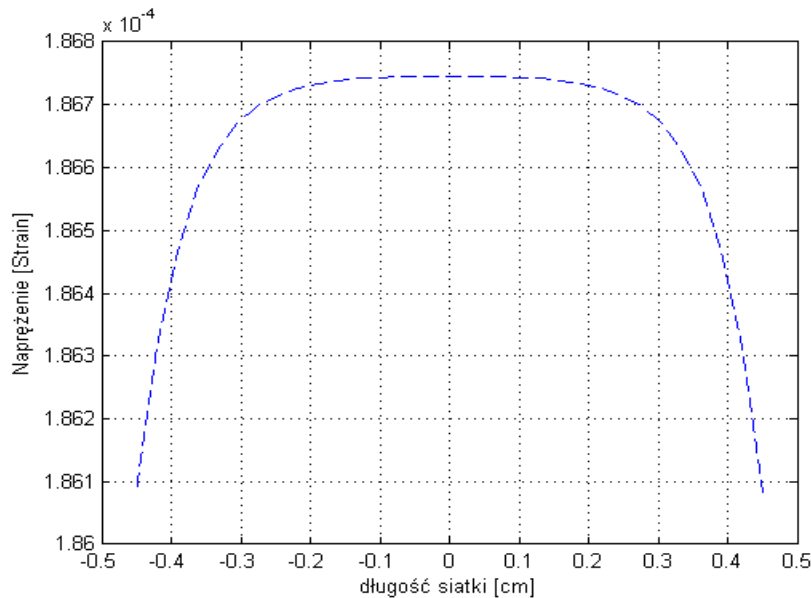


Figure 6. The elongation distribution calculated using BEM

The maximum value of the absolute error of the elongation determination was $RMSD = 0.0092\%$ for MES and $RMSD = 0.0085\%$ for BEM. It was calculated by accounting for the division of the grating into 10 sections using the following equation:

$$RMSD = \left(\frac{1}{10} \cdot \sum_{k=1}^5 \varepsilon_C - \varepsilon_M \right)^{1/2}, \quad (10)$$

This error was determined as the root square error and defines the difference between the calculated values of the elongation ε_C and the values obtained using the conjugate gradient algorithm ε_M .

IV. CONCLUSIONS

The results of laboratory measurements and numerical calculations show that it is possible to apply the inverse analysis to determine the distribution of elongation using fiber optic sensors with Bragg gratings. It is possible to perform calculations using numerical algorithms performing calculations in accordance with the mathematical structure of the FBG model and taking into account the values of all model parameters. The boundary element and finite element method used in this paper, allows to obtain comparable results for the indirect measurement.

REFERENCES

[1] H. Fujii, T. Namazu, S. Inoue, R. Dembo, D. Rosen, "Development of the Novel Elongation-Measurement Device with In-Plane Bimorph Actuator for the Tensile Test," *Micro Electro Mechanical Systems 2009, MEMS 2009. IEEE 22nd International Conference on*, pp. 1063-1066, 2009.

[2] A. Granda, F. M. F. Linera, G. Vecino, A. Diaz Canga, "Practical Speed and Elongation Measurement, Using Encoders, for a Temper Mill," *Industry Applications, IEEE Transactions on*, vol. 50(1), pp. 113-119, 2009.

[3] M. Szustakowski, N. Palka, B. Kizlik, "Contrast of the Fiber optic Michelson interferometer – a new prospect for elongation measurement," *Modern Problems of Radio Engineering,*

Telecommunications and Computer Science, Proceedings of International Conference IEEE, pp. 476-477, 2004.

[4] A. Wolff, D. Cramer, H. Hellebrand, I. Probst, K. Lubitz, "Optical two channel elongation measurement of PZT piezoelectric multilayer stack actuators," *Applications of Ferroelectrics, 1994. ISAF '94. Proceedings of the Ninth IEEE International Symposium on*, pp. 755-757, 1994.

[5] R. K. Yamashita, W. Zou, Z. He, K. Hotate, "Measurement Range Elongation Based on Temporal Gating in Brillouin Optical Correlation Domain Distributed Simultaneous Sensing of Strain and Temperature," *Photonics Technology Letters, IEEE* vol. 24(12), pp. 1006-1008, 2012.

[6] E. Roger, A. Khayat, L. A. Utracki, F. Godbille, J. Picot, "Influence of shear and elongation on drop deformation in convergent-divergent flows", *International Journal of Multiphase Flow*, vol. 26(1), pp. 17-44, 2000.

[7] U. Iturraran-Viveros, F. J. Sanchez-Sesma, F. Luzon, "Boundary element simulation of scattering of elastic waves by 3-D cracks," *Journal of Applied Geophysics* vol. 64(3-4), pp. 70-82, 2008.

[8] Y. Liu, N. Nishimura, Y. Otani, "Large-scale modeling of carbon-nanotube composites by a fast multipole boundary element method," *Computational Materials Science*, vol. 34(2), pp. 173-187, 2005.

[9] S. Chatelin, C. Deck, F. Renard, S. Kremer, C. Heinrich, J. P. Armspach, R. Willinger, "Computation of axonal elongation in head trauma finite element simulation," *Journal of the Mechanical Behavior of Biomedical Materials*, vol. 4(8), pp. 1905-1919, 2011.

[10] Y. B. Fu, C. K. Chui, "Modelling and simulation of porcine liver tissue indentation using finite element method and uniaxial stress-strain data," *Journal of Biomechanics*, vol. 47(10), pp. 2430-2435, 2014.

[11] E. Lin, H. Chen, Y. Liu, "Finite element implementation of a non-local particle method for elasticity and fracture analysis," *Finite Elements in Analysis and Design*, vol. 93, pp. 1-11, 2015.

[12] M. Hadjicharalambous, J. Lee, N. P. Shith, D. A. Nordsletten, "A displacement-based finite element formulation for incompressible and nearly-incompressible cardiac mechanics," *Computer Methods in Applied Mechanics and Engineering*, vol. 274, pp. 213-236, 2014.

[13] P. Kisała, "Measurement of the maximum value of non-uniform strain using a temperature-insensitive fibre Bragg grating method," *Optoelectronics Review* vol. 21(3), pp. 293-302, 2013

[14] P. Kisała, "Metrological conditions of strain measurement optoelectronic method by the use of fibre Bragg gratings," *Metrology and Measurement Systems* vol. 19(3), pp. 471-480, 2012.

[15] M. Czerwiński, J. Mroccka, T. Girasole, G. Gouesbet, G. Grehan, "Light-Transmittance Predictions Under Multiple-Light Scattering Conditions. I. Direct Problem: hybrid-Method Approximation," *Applied Optics* vol. 51(11), pp. 1715-1723, 2012.

[16] J. Mroccka, D. Szczuczyński, "Improved regularized solution of the inverse problem in turbidimetric measurements," *Applied Optics* vol. 49(24), pp. 4591-4603, 2010.

- [17] J. Mroczka, D. Szczuczyński, "Improved regularized solution of the inverse problem in turbidimetric measurements," *Applied Optics* vol. 49(24), pp. 4591-4603, 2010.
- [18] P. Kisała, "Generation of a zone chirp in uniform Bragg grating as a way of obtaining double functionality of a sensor," *Metrology and Measurement Systems* vol. 19(4), pp.727-738, 2012
- [19] J. Mroczka, "The cognitive process in metrology," *Measurement* vol. 46(8), pp. 2896-2907, 2013.
- [20] S. Ciężczyk, "Passive Open-Path FTIR Measurements and Spectral Interpretations for in situ Gas Monitoring and Process Diagnostics," *Acta Physica Polonica A* 126(3), pp. 673-678, 2014.
- [21] S. Ciężczyk, "Non-Luminous Flame Temperature Determination Method Based on CO₂ Radiation Intensity," *Acta Physica Polonica A* 126(6), pp. 1235-1240, 2014
- [22] G. Świrniak, G. Głomb, J. Mroczka, "Inverse analysis of the rainbow for the case of low-coherent incident light to determine the diameter of a glass fiber," *Applied Optics* vol. 19(1), pp. 4239-4247, 2014.